Inorganic Chemistry Research

Article

Voltammetric and Amperometric Determination of Iodate Using Ionic Liquid/Polyoxotungstate/MWCNTs-COOH Organic-Inorganic Nanohybrid Modified Glassy Carbon Electrode

Atefeh Karimi-Takallo and Somayeh Dianat*

Department of Chemistry, Faculty of Sciences, University of Hormozgan, Bandar Abbas 79161-93145, Iran.

Received: May 21, 2021; Accepted: August 3, 2021
Cite This: *Inorg. Chem. Res.* **2021,** *5*, 215-223. DOI: 10.22036/icr.2021.287225.1103

In this study, a nanohybrid modified glassy carbon electrode (GCE) was successfully fabricated with a tri-component nanocomposite consisting of (1,1'-(1,4-Butanediyl) dipyridinium) ionic liquid (bdpy), $PW_{11}O_{39}Co(H_2O)$ ($PW_{11}Co$) polyoxometalate (POM), and carboxyl functionalized multi-walled Carbon Nanotubes (MWCNTs-COOH) by drop-casting, followed by electrodeposition technique. The morphological, electrochemical, and electrocatalytic properties of the (bdpy)$PW_{11}Co$/MWCNTs-COOH/GCE were investigated by field emission scanning electron microscopy (FE-SEM) combined with energy-dispersive X-ray spectroscopy, voltammetry, and amperometry methods. The FE-SEM images well showed immobilization of (bdpy)$PW_{11}Co$/MWCNTs-COOH on GCE through deformation of the mirror surface to the rough surface. The electrochemical test results confirmed that modified electrode has high stability and remarkable electrocatalytic behavior toward the reduction of iodate ion. The proposed sensor displayed two linear ranges of 10.0-200.0, and 200.0-1600.0 µmol L^{-1} with LOD of 27.6×10^{-2} µmol L^{-1} (S/N=3), and sensitivity of 41.0 µA mmol L^{-1}, and 20.0 µA mmol L^{-1}, respectively, by amperometry method. Moreover, the results of the electrochemical experiments indicated that this sensor has excellent selectivity, good reproducibility, repeatability, and analytical performance in real samples.

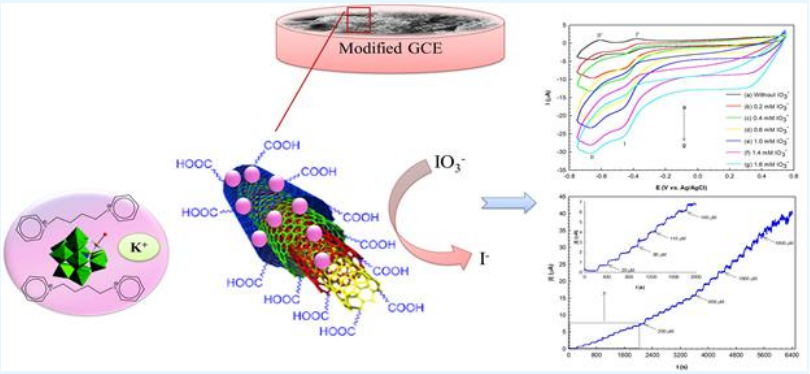

Keywords: Ionic liquid, Polyoxometalate (POM), Electrodeposition method, Electrocatalysis, Iodate determination

1. INTRODUCTION

Polyoxometalates (POMs) are a large class of anionic nanoclusters containing early transition metals and oxygen atoms to form a closed three-dimensional (3D) framework.[1,2] POMs, especially Keggin-type POMs, have different applications in the fields of catalysis,[3-6] medicine,[7-9] and molecular materials[10,11] due to their excellent redox character, unique molecular structure, electronic versatility, and easy preparation. One of the attractive properties of POMs is that the anionic cluster can undergo a fast, stepwise, reversible, and multi-electron transfer reaction while keeping the structural integrity.[1,12-14] The multiple redox properties make them attractive candidates in surface modification, electroanalysis, and electrocatalysis.[1,12,13,15]

Different methods have been developed to achieve chemically modified electrodes (CMEs) with POMs such as electrodeposition at a very negative potential,[16,17] adsorption,[18] entrapment into conducting,[19,20] or non-conducting polymers matrixes,[21,22] layer-by-layer self-assembly,[23,24] Langmuir-Blodgett (LB) technique,[25,26] preparation of self-assembled monolayer and multilayer thin-films,[27] and bulk modification of carbon composites and carbon paste matrices.[28] However, the electrocatalytic activity of POMs-modified electrodes is limited due to their low stability in aqueous solutions[15,27,29] and low specific surface area.[30]

To achieve the enhanced stability of POMs, many studies have been focused on the design and construction of modifying and assemble POMs with suitable organic matrices, which is one of the most exciting fields in

materials chemistry.[27,31-33] Recently, ionic liquids (ILs) have concerned more attention,[34-36] due to owning highlight properties such as good aqueous solubility, high electrical conductivity, non-volatility, non-flammability, low toxicity, high thermal and electrochemical stabilities, and large electrochemical potential window.[37]

Furthermore, immobilization or dispersion of POMs on different supporting carbon materials has attracted significant attention due to their small background currents, wide potential windows, low-cost, excellent chemical stability, and a strong affinity for POMs.[38-43]

In the past decade, carbon nanotubes (CNTs) had been used for improving the electrocatalytic activity of the modified electrodes due to their unique chemical and physical properties.[44-46] Also, CNTs are favorable support for POM-based catalysts due to their outstanding structural, mechanical, and electronic properties.[47-49] CNTs are included single-walled carbon nanotubes (SWCNTs) and multi-walled carbon nanotubes (MWCNTs), which have attracted researchers' attention in the field of physics, chemistry, and material science since their discovery by Sumio Iijima in 1991.[50] MWCNTs are very promising candidates as an electrocatalyst in analytical and material science, due to their large specific surface area, excellent chemical/physical stability, wide electrochemical windows, and ultra-high electrical conductivity.[41,42,51-53]

Lately, different POM-based electrocatalysts have concerned much attention due to their unique physical and chemical properties. Manivel *et al.* reported a silver nanoparticle-embedded polybenzidine matrix containing phosphomolybdic acid (Ag/PMo_{12}/PBz) modified GCE for the electrochemical detection of chlorate, bromate, and iodate ions in aqueous solutions.[54] Zhang *et al.* developed a composite modified electrode based on attapulgite/polyaniline/phosphomolybdic acid (attapulgite/PANI/PMo_{12}/GCE) for the detection of iodate.[55] Zuo *et al.* reported a sensor for the iodate determination based on $K_{28}Li_5H_7[P_8W_{48}O_{184}]_{92}H_2O$ (P_8W_{48}) and Cu@AgNPs composite film.[56] Sharifi et al. fabricated a novel modified GCE based on tetra-component nanocomposite consisting of (1,1'-(1,4-Butanediyl) dipyridinium) ionic liquid (bdpy), $SiW_{11}O_{39}Ni(H_2O)$ ($SiW_{11}Ni$) Keggin-type polyoxometalate (POM), and phosphorus-doped electrochemically reduced graphene oxide (P-ERGO) by electrodeposition technique. Then, they investigated electrochemical and electrocatalytic behaviors, of the proposed sensor for iodate (IO_3^-) determination.[57]

In this study, K(1,1'-(1,4-Butanediyl)dipyridinium)$_2$[$PW_{11}O_{39}Co(H_2O)$]/carboxyl functionalized multi-walled carbon nanotubes ((bdpy)PW_{11}Co/MWCNTs-COOH) organic-inorganic nanocomposite has been processed on a glassy carbon electrode (GCE) by electrodeposition method. Then, electrochemical and electrocatalytic behaviors, selectivity, repeatability, reproducibility of the proposed sensor for iodate (IO_3^-) determination, and also the recovery in the mineral water, and tap water were investigated. The suggested strategy for the renovation of PW_{11}Co by bdpy ionic liquid and MWCNTs-COOH displays notable benefits, which should be essential for practical application.

2. EXPERIMENTAL

Material and reagents

The (bdpy)PW_{11}Co/MWCNTs-COOH was prepared according to the previous literature.[58] Tungstophosphoric acid ($H_3PW_{12}O_{40}$, abbreviated as HPW), cobalt(II) acetate tetrahydrate ($(CH_3COO)_2Co.4H_2O$), potassium acetate (CH_3COOK), glacial acetic acid (CH_3COOH), potassium hydrogen carbonate ($KHCO_3$), 1,1'-(1,4-Butanediyl)dipyridinium dibromide (bdpy) ionic liquid, sodium perchlorate ($NaClO_4$), potassium hexacyanoferrate (III) ($K_3[Fe(CN)_6]$), and potassium iodate (KIO_3) were of analytical grade and obtained from Merck or Sigma companies. All reagents were used as received without any more purification. MWCNTs-COOH (>95% purity, length ~ 30 µm, ID = 5-10 nm, OD = 10-20 nm, COOH content = 2.00 wt%, and SSA = 200 m^2 g^{-1}) were purchased from Tecnan company, (Spain). All solutions were prepared with deionized water (DI, 18 MΩ cm (25 °C), Milli Q, Millipore Inc.).

Analytical measurements

ATR-FTIR spectra were collected on a PerkinElmer Spectrum Two in a wavenumber range of 2400-400 cm^{-1}. UV-Vis absorption spectra were monitored with a Unico SQ 4802 UV-Vis spectrophotometer- double beam with a 1.0 cm path length cell. The crystal structures of the PW_{11}Co, bdpy, (bdpy)PW_{11}Co, MWCNTs-COOH, and (bdpy)PW_{11}Co/MWCNTs-COOH were studied by XRD (Panalytical X' Pert Pro X-ray diffractometer, The Netherlands) with Cu Kα radiation.

TGA/DTA measurements were done under airflow while gradually increasing the temperature with a rate of 10 °C min^{-1}, using a Rheometric Scientific STA 1500 for samples up to 800 °C. The percent of immobilized (bdpy)PW_{11}Co on the MWCNTs-COOH was determined from inductively coupled plasma-optical emission spectrometry (Optima 7300 V ICP-OES spectrometer Brochure-PerkinElmer) by measuring tungsten contents in (bdpy)PW_{11}Co/MWCNTs-COOH.

The structure and morphology of the (bdpy)PW_{11}Co/MWCNTs-COOH were compared with MWCNTs-COOH by TEM (EM10C-100 kV series, Zeiss Co., Germany). The morphology of the bare GCE and (bdpy)PW_{11}Co/MWCNTs-COOH/GCE were investigated using FE-SEM (SIGMA VP, Zeiss Co., Germany), equipped with energy-dispersive X-ray spectrometry (EDS) and EDS-mapping.

Electrochemical measurements

The electrochemical tests were taken with an Autolab P/GSTAT 302N instrument (GPES 4.9, Eco-Chemie Utrecht, The Netherlands) in a conventional three-electrode glass cell containing bare or modified GCE (GR-2S/N, Iran, Tehran, diameter 2.0 mm), a Pt rod (IV-EL/EB-2200, Ivium, Eindhoven, The Netherlands) and an Ag/AgCl (3.0 mol L^{-1} KCl) electrode

(Metrohm, Switzerland) as working, counter and reference electrodes, respectively. To eliminate the dissolved oxygen influence on the iodate determination, pure argon gas (99.999%) was bubbled into the electrolytic cell solutions for 15 minutes prior to the electrochemical experiments and blanketed by the argon atmosphere during the experiments. All of the experiments were carried out at ambient temperature.

Pretreatment of GCE

The GCE was cleaned by polishing with α-Al_2O_3 slurries (0.30, 0.10, and 0.05 μm) on a micro cloth pad to obtain a flat and mirror surface followed by sonication in H_2O, CH_3Cl, and H_2O bath respectively, each for 5-minute. Then the GCE was cleaned electrochemically by repeated cycling in H_2SO_4 (0.5 mol L^{-1}) in the potential range of -1.0 to 1.0 V versus Ag/AgCl (3.0 mol L^{-1} KCl) until stable voltammograms were achieved. Finally, the GCE was thoroughly rinsed with DI water and dried naturally at ambient temperature.

Preparation of (bdpy)PW_{11}Co/MWCNTs-COOH/GCE

The electrode modification was performed in various steps (Scheme 1) according to our previous literature.[58] In summary, First, 5.0 μL of the synthesized (bdpy)PW_{11}Co/MWCNTs-COOH suspension was dropped onto the polished bare GCE using a micropipette, dried under an infrared lamp (250 W) for 30 minutes, and washed with deionized water. Then, the prepared GCE was exposed to twenty cycles of CV in the potential range of 0 to -1.4 V at a scan rate of 0.025 V s^{-1} in a suspension of (bdpy)PW_{11}Co/MWCNTs-COOH (1.0 mg mL^{-1}) containing sodium perchlorate (24.5 mg mL^{-1}). The modified electrode was signified as (bdpy)PW_{11}Co/MWCNTs-COOH/GCE through the text. For comparison, the same procedure was operated to make PW_{11}Co/GCE, bdpy/GCE, and (bdpy)PW_{11}Co/GCE.

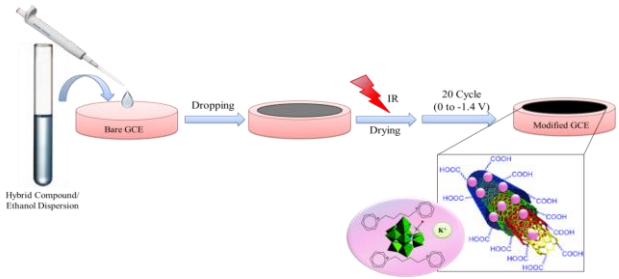

Scheme 1. Stepwise procedure for the electrode modification.[58]

3. RESULTS AND DISCUSSION

Characterization

The elemental analysis, ATR-FTIR spectra, UV-Vis absorption spectroscopy, XRD, TGA/DTA, and TEM of prepared nanocomposite material were investigated in the previous study[58] and the results are shown in the supporting information. The ATR-FTIR, UV-Vis, XRD, TGA/DTA, and TEM analysis were shown in Figures 1S-A, 1S-B, 2S, 3S, and 4S, respectively.

Generally, the (bdpy)PW_{11}Co, and (bdpy)PW_{11}Co/MWCNTs-COOH characterizations showed that without a change in the basic Keggin structure of PW_{11}Co, the bdpy is functionalized on the PW_{11}Co, and (bdpy)PW_{11}Co is immobilized on the MWCNTs-COOH.

Surface morphology and energy dispersive analysis of X-ray spectroscopy (EDS) measurement of (bdpy)PW_{11}Co/MWCNTs-COOH/GCE

The morphologies of the bare GCE and (bdpy)PW_{11}Co/MWCNTs-COOH/GCE were investigated by field emission scanning electron microscopy (FE-SEM), according to our previous literature.[58] The FE-SEM images of the bare GCE (Figure 1A, image (a, b)) have mirror and homogeneous surface which were reformed to rudely and heterogeneously surface after the immobilization of (bdpy)PW_{11}Co/MWCNTs-COOH on GCE (Figure 1B, image (a, b)). Moreover, Figures 1A and B (c) display the EDS of the bare GCE and (bdpy)PW_{11}Co/MWCNTs-COOH/GCE, respectively. The EDS spectra and elemental mappings confirm the elemental composition, which discloses the existence of C, and O in the bare GCE (Figure 1A, images c-e), and C, W, O, P, N, Co, and K elements on the modified GCE (Figure 1B, images (c-j)). These results confirmed the immobilization of the (bdpy)PW_{11}Co/MWCNTs-COOH on the GCE.

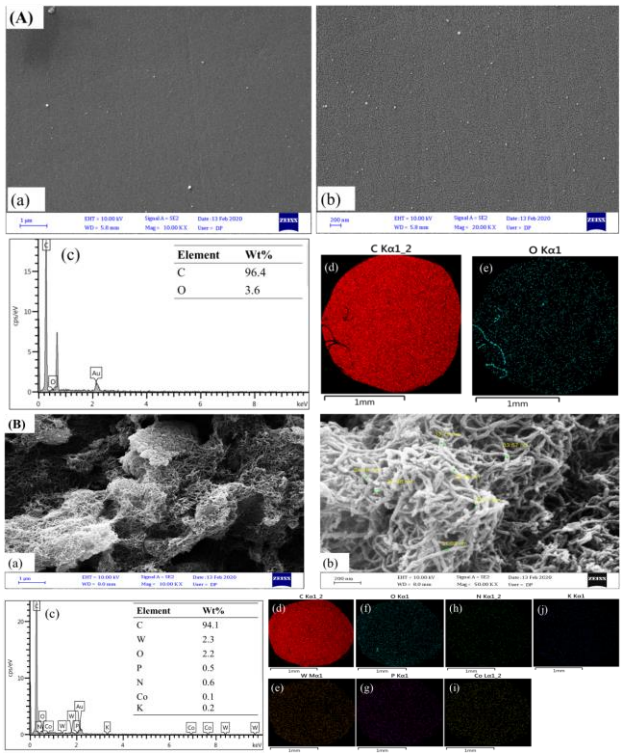

Figure 1. (A) FE-SEM images (a, b), EDS pattern (c), and EDS element mapping (d, e) of the bare GCE and (B) FE-SEM images (a, b), EDS pattern (c) and EDS element mapping (d-j) of (bdpy)PW_{11}Co/MWCNTs-COOH/GCE.[58]

Electrochemical characterization of (bdpy)$PW_{11}Co$/MWCNTs-COOH/GCE

POMs can undergo a reversible multi-electron redox process after immobilization on the electrode surface. So, in our previous study, the different electrochemical methods such as cyclic voltammetry (CV) in $HClO_4$ (0.1 mol L^{-1}, pH 1.5), and $K_3Fe(CN)_6$ (0.5 mmol L^{-1}) aqueous solutions were applied to confirm the development of the prepared (bdpy)$PW_{11}Co$/MWCNTs-COOH/GCE.[58] The electrochemical study of this modified surface was performed in an aqueous solution with acidic pH because POMs decompose in neutral and basic conditions.[60] Moreover, the active surface area of the modified electrode in $K_3Fe(CN)_6$ (0.5 mmol L^{-1}, pH 3) was also measured. Results of these experiments are shown in the supporting information section (Figures 5S, and 6S).

The results presented the evidence that the (bdpy)$PW_{11}Co$/MWCNTs-COOH/GCE has two pairs of pseudo-reversible index redox peaks that were ascribed to the two sequential one-electron processes relating to $W^{VI} \rightarrow W^{V} \rightarrow W^{IV}$.

Furthermore, the electrochemical measurements verify that the (bdpy)$PW_{11}Co$/MWCNTs-COOH/GCE displays better redox behavior compared with the $PW_{11}Co$/GCE, bdpy/GCE, and MWCNTs-COOH/GCE due to the synergistic effect between these tri-blocks, which is very advantageous for electrocatalytic applications. Additionally, this phenomenon means that MWCNTs-COOH support can increase the effective surface area of the modified electrode and facilitate the electron transfer between the GCE and (bdpy)$PW_{11}Co$ in a most effective path.

Electrocatalytic properties of (bdpy)$PW_{11}Co$/MWCNTs-COOH/GCE

The electrocatalytic activity of the (bdpy)$PW_{11}Co$/MWCNTs-COOH/GCE for IO_3^- electro-reduction was investigated by CV technique in 0.1 mol L^{-1} $HClO_4$ aqueous solution (pH = 1.5) containing different concentrations of IO_3^- (Figure 2). With the increasing concentrations of IO_3^-, the cathodic peak current at about -0.450 V (Peak I) of the nanocomposite modified electrode gradually increased, whereas the corresponding oxidation peak current decreased, suggesting that (bdpy)$PW_{11}Co$/MWCNTs-COOH/GCE would have a potential ability in the detection of IO_3^-. However, the CV method, due to essential defects such as low sensitivity and a high limit of detection (LOD), is insufficient for quantitative chemical analysis. Therefore, differential pulse voltammetry (DPV) and amperometry techniques, which benefit from low LOD and high sensitivity (small influence of background in analytical signal), were used for the sensitive measurement of IO_3^- at (bdpy)$PW_{11}Co$/MWCNTs-COOH/GCE.

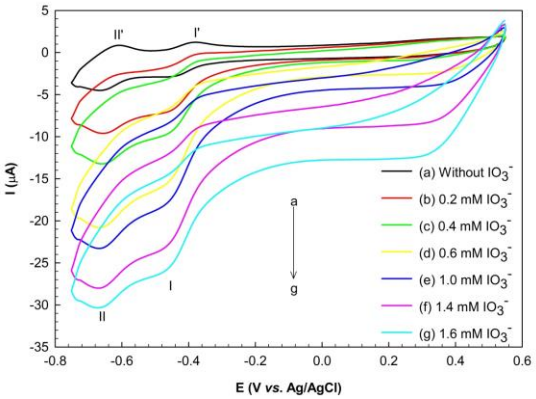

Figure 2. CVs of the (bdpy)$PW_{11}Co$/MWCNTs-COOH/GCE with different concentrations of IO_3^- in $HClO_4$ aqueous solution (0.1 mol L^{-1}, pH 1.5); scan rate 100 mV s^{-1}.

Determination of IO_3^- by DPV

The DPV responses to IO_3^- of the (bdpy)$PW_{11}Co$/MWCNTs-COOH/GCE in 0.1 mol L^{-1} $HClO_4$ (pH = 1.5) were recorded in Figure 3. Calibration curve for quantification of IO_3^- was obtained by plotting the dependence of peak I current *vs.* concentration of IO_3^- ($[IO_3^-]$) under optimum experimental conditions (inset of Figure 3). The proportional increase of the i_p values with increasing $[IO_3^-]$ was observed in the two linear ranges of 1.0-4.0 μmol L^{-1} and 4.0-20.0 μmol L^{-1} with linear regression equations of i_p (μA) = 11.7 × $10^{-2}[IO_3^-]$ (μmol L^{-1}) + 1.20 (R^2 = 0.996), and i_p (μA) = 5.0 × 10^{-3} $[IO_3^-]$ (μmol L^{-1}) + 1.65 (R^2 = 0.969), limit of detection (LOD, S/N = 3) of 10.4 × 10^{-2} μmol L^{-1}, limit of quantitation (LOQ, S/N = 10) of 34.7 × 10^{-2} μmol L^{-1}. The LOD and LOQ were estimated by using the following equations, LOD = $3S_b/m$, and LOQ = $10S_b/m$, where S_b is the standard deviation of twenty responses of the blank solution and m is the slope of the regression line.

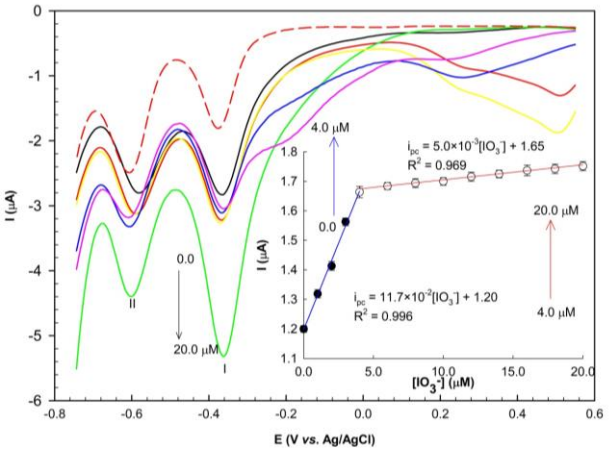

Figure 3. DPV responses for the determination of IO_3^- in the concentration ranges of 0.0-20.0 μmol L^{-1} in $HClO_4$ aqueous solution (0.1 mol L^{-1}, pH 1.5) at (bdpy)$PW_{11}Co$/MWCNTs-COOH/GCE. The inset shows calibration plot for IO_3^- determination (peak I). Parameters: step potential = 6.0 mV, Amplitude potential = 50.0 mV.

Determination of IO_3^- by amperometry

Amperometry was also applied to examine the sensing characteristics of the (bdpy)$PW_{11}Co$/MWCNTs-COOH/GCE for determination of IO_3^- (Figure 4A). As the IO_3^- was added into the stirred 0.1 mol L^{-1} $HClO_4$ aqueous solution at an optimum potential of -0.400 V, dynamic stairs of the current with quick steady-state were obtained, and the currents increased along with the continuous addition of IO_3^-. This can be due to the rapid diffusion of the IO_3^- small molecules from the solution to the surface of the modified electrode and the better electron transfer rate of the modifier, which can play an important role. The calibration curve presented in Figure 4B indicated that IO_3^- sensor based on (bdpy)$PW_{11}Co$/MWCNTs-COOH/GCE displayed two linear response range from 0.0 to 200.0 µmol L^{-1} and 200.0 to 1600.0 µmol L^{-1} with linear regression equations of i_p (µA) = 4.1 × 10^{-2} [IO_3^-] (µmol L^{-1}) + 0.097 (R^2 = 0.994), and i_p (µA) = 2.0 × 10^{-2}[IO_3^-] (µmol L^{-1}) + 4.02 (R^2 = 0.998), LOD of 27.6 × 10^{-2} µmol L^{-1}, LOQ of 92.1 × 10^{-2} µmol L^{-1}, and sensitivity of 41.0 µA mmol L^{-1}, and 20.0 µA mmol L^{-1}. However, at higher concentrations of 1600.0 µmol L^{-1}, the noise of the amperometric signal increases, and the current stabilization takes longer and longer until no straight line is achieved anymore.

The linear calibration range, LOD, and sensitivity of the suggested sensor for IO_3^- determination are compared with those in previous literatures (Table 1).[54-57,59-67] The results proved that (bdpy)$PW_{11}Co$/MWCNTs-COOH/GCE is an excellent platform for IO_3^- detection.

The structure of $PW_{11}O_{39}Co(H_2O)$, due to its electron transfer properties within the cluster can be in either form $H_4PW_4^{V}W_7^{VI}Co(H_2O)O_{39}^{5-}$ or $H_6PW_6^{V}W_5^{VI}Co(H_2O)O_{39}^{5-}$. Both of these structures can similarly reduce IO_3^- to I^-. Therefore, the electrocatalytic behavior of the nanocomposite modified GCE towards IO_3^- can be explained by the following mechanisms (1 or 2), that is according to previous literature:[57,59,60]

$$3H_4PW_4^{V}W_7^{VI}Co(H_2O)O_{39}^{5-} + IO_3^- \rightarrow 3H_2PW_2^{V}W_9^{VI}Co(H_2O)O_{39}^{5-} + I^- + 3H_2O \quad (1)$$

$$3H_6PW_6^{V}W_5^{VI}Co(H_2O)O_{39}^{5-} + IO_3^- \rightarrow 3H_4PW_4^{V}W_7^{VI}Co(H_2O)O_{39}^{5-} + I^- + 3H_2O \quad (2)$$

Stability, repeatability, and reproducibility of the (bdpy)$PW_{11}Co$/MWCNTs-COOH/GCE

Achieving a sensor, biosensor, and/or bioreactor with high stability is one of the most important goals of analytical electrochemistry. POMs-modified electrodes are usually unstable in aqueous solutions because POMs can easily leach out from the electrode surface into the electrolyte. The stability of the (bdpy)$PW_{11}Co$/MWCNTs-COOH/GCE was investigated under potential cycling by recording successive CVs in 0.1 mol L^{-1} $HClO_4$ solution (pH 1.5) at 100 mV s^{-1}, according to our previous literature[58], and monitoring the changes in peak currents. As is shown in Figure 5A, the cathodic and anodic peak currents of the (bdpy)$PW_{11}Co$/MWCNTs-COOH/GCE display a slight change after 220 cycles of CV scan. The peak I current value remains about 85.0% of the first value after 220 cycles. The variations of peak I currents with scan numbers have been plotted and shown in the inset of Figure 5A. Additionally, the long-term stability experiment was also performed by keeping the (bdpy)$PW_{11}Co$/MWCNTs-COOH/GCE in the air at ambient conditions. The results showed that the peak I current of the modified electrode stayed at 95.3 % of its primary current after ten days, 94.6% after 20 days, and 90.7% after one month, indicating the excellent long-term stability of the suggested sensor (Figure 5B). The excellent stability of the (bdpy)$PW_{11}Co$/MWCNTs-COOH/GCE can be attributed to the presence of bdpy and MWCNTs-COOH in the mentioned nanocomposite structure, which reduces its solubility in aqueous solutions.

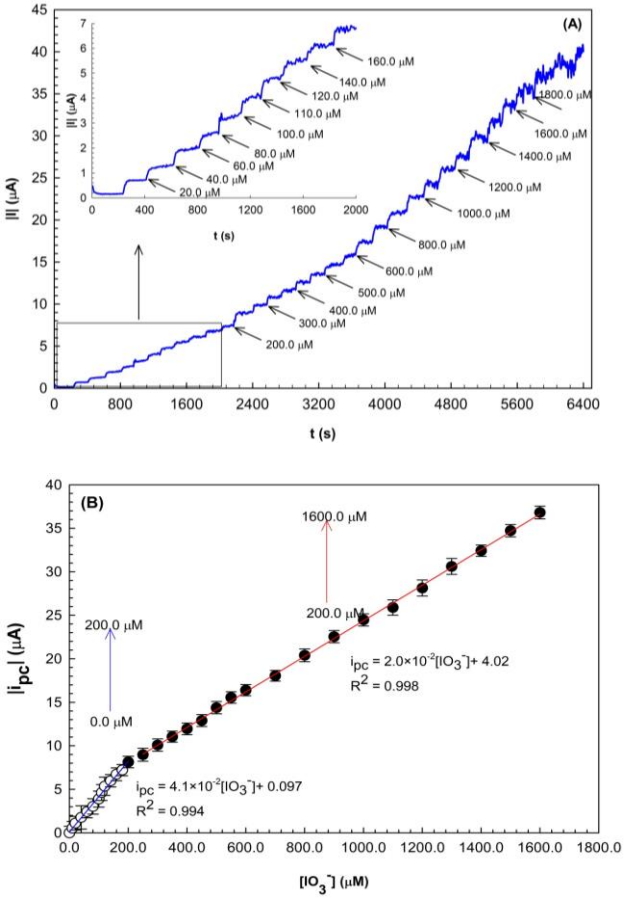

Figure 4. (A) Current-time responses of (bdpy)$PW_{11}Co$/MWCNTs-COOH/GCE in $HClO_4$ aqueous solution (0.1 mol L^{-1}, pH 1.5) at -0.400 V with an increasing of IO_3^- concentration. (B) Corresponding calibration plot of the absolute value of steady-state currents obtained against concentrations of IO_3^-.

Table 1 Comparative characteristics of the proposed sensor and some other electrodes for the determination of IO_3^-

Modified Electrode	Sweep mode	Linear range (μM)	LOD (μM)	Sensitivity (μA mM^{-1})	Ref.
PMo_{12}-doped sol-gel film on GCE	Amperometry	5-6000	1	8	[59]
$CoW_{11}Co/PVP^a/TiO_2$/GCE	Amperometry	2-280	0.8	N.R.[b]	[60]
Fe(III)P-MWCNTs-GCE	Amperometry	10-4000	2.5	1.5	[61]
P_2Mo_{18}/OMC^c/GC	Amperometry	1.13-6250	0.377	1.51	[62]
PMo_{12} modified CILE[d] using $[C_8Py][PF_6]$	Amperometry	10-1000	2.6	6.3	[63]
GCE/MWCNTs/$[C_8Py][PF_6]$-PMo_{12}	Amperometry	20-200	15	14	[64]
Ag/PMo_{12}/PBz^e/GCE	Amperometry	N.R.	1.45	0.57	[54]
Attapulgite/$PANI^f/PMo_{12}$/GCE	Amperometry	2-520	0.53	300	[55]
$[PEI^g/PSS^h$-Cu@AgNPs/PEI/$P_8W_{48}]_5$/ITO^i	Amperometry	0.1-300	0.04	5.52	[56]
Fe(II)-$NClin^j$-CPE^k	SWV	4-100	0.64	67	[65]
Carbon nanoparticles-poly(ortho-aminophenol)-modified electrode	Amperometry	500-6500	10	17.14	[66]
$PdNF^l/TiO_2NT^m$/Ti	Amperometry	8.0-95.2	3.4	8.5×10^3	[67]
		95.2-666.6		5.0×10^2	
		666.6-2065.0		1.0×10^2	
(bdpy)SiW_{11}Ni/P-ERGO/GCE	SWV	10-400	2.4×10^{-3}	5.50	[57]
		400-1000		1.40	
	Amperometry	10-1600	4.7×10^{-4}	28.10	
(bdpy)PW_{11}Co/MWCNTs-COOH/GCE	DPV	0.0-4.0	10.4×10^{-2}	109.0	This
		4.0-20.0		5.1	work
	Amperometry	10.0-200.0	27.6×10^{-2}	41.0	
		200.0-1600.0		20.0	

[a]Poly (4-vinylpyridine). [b]N.R. Not recorded. [c]Ordered mesoporous carbon. [d]Carbon ionic liquid electrode. [e]Polybenzidine. [f]Polyaniline. [g]Poly (ethylenimine). [h]Poly (sodium-p-styrenesulfonate). [i]Indium tin oxide. [j]Clinoptilolite nanoparticles. [k]Carbon paste electrode. [l]Palladium nanoflowers. [m]Titanium oxide nanotubes.

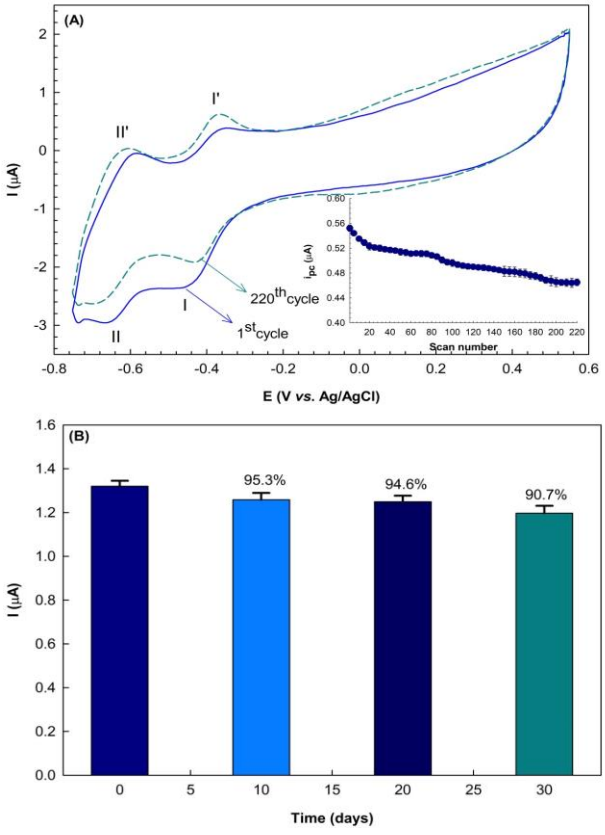

Figure 5. (A) Stability investigation under potential cycling of (bdpy)PW_{11}Co/MWCNTs-COOH/GCE in $HClO_4$ (0.1 mol L^{-1}, pH 1.5) over 220 scans at the scan rate of 100 mV s^{-1}. The inset shows variations of the cathodic peak I currents versus the potential scan numbers.[58] (B) Long-term stability of (bdpy)PW_{11}Co/MWCNTs-COOH/GCE in $HClO_4$ (0.1 mol L^{-1}, pH 1.5) during 30 days.

To validate the repeatability of the (bdpy)PW_{11}Co/MWCNTs-COOH/GCE, five different experiments with one modified GCE surface were repeated in the presence of IO_3^- (50.0 μmol L^{-1}). Furthermore, five (bdpy)PW_{11}Co/MWCNTs-COOH/GCE were prepared under the same conditions to compare the response currents of IO_3^-. The values of relative standard deviation (RSD) of the response currents for the repeatability and reproducibility were 0.330% and 0.320%, respectively, which demonstrated that the modified electrode has excellent repeatability and reproducibility.

Interference study

The selective response is an essential characteristic for sensors that probe the sensor-selective response to an analyte in the presence of other species. For this purpose, the potential interferences for the IO_3^- detection on this sensor were studied by adding various potential interferents into $HClO_4$ (0.1 mol L^{-1}, pH 1.5) aqueous solution using the differential pulse voltammetry (DPV) technique. As displayed in Table 2, no significant response was observed for each excessive addition of Cl^-, I^-, and $S_2O_3^{2-}$ at 5.0 times, NO_2^-, and PO_4^{3-} at 2.0 times, and NO_3^- at a concentration equal to the concentration of IO_3^-.

Table 2. Effect of interference ions on the detection of IO_3^- (15.0 μmol L^{-1})

Interference ions	$\frac{[Interference\ ion]}{[IO_3^-]}$	Relative signal change (%)
Cl^-	5.0	+5.7
I^-	5.0	+1.5
NO_2^-	2.0	+3.5
NO_3^-	1.0	+2.4
PO_4^{3-}	2.0	+1.0
$S_2O_3^{2-}$	5.0	+1.2

Analytical applications for real sample

The analytical applicability of the prepared (bdpy)$PW_{11}Co$/MWCNTs-COOH/GCE was validated based on the determination of iodate concentration in mineral water (Damavand Mineral Water Co., Iran), and tap water. The real samples were directly prepared in the $HClO_4$ solution (0.1 mol L^{-1}, pH = 1.5) without further treatment. The content of iodate in the solution was determined by the iodometric titration method as a standard method according to the procedure given in the previous literature.[68] The measurements were performed using the standard addition method, by DPV response method. The voltammetric measurements were performed at the applied potential of about -0.370 V, equilibration time, 5 s; step potential, 0.006 V; pulse amplitude, 0.050 V; initial potential, 0.550 V; and end potential, -0.750 V. The standard solutions of iodate were injected into the real samples to check the recovery percent of added iodate (Found value/Intrinsic value). As shown in Table 3, the obtained results are in good agreement with the results of the standard method with high accuracy and precision (recovery close to 100%). Therefore, the proposed modified electrode can be efficiently applied in detecting trace-level IO_3^- in real samples.

Table 3. Recovery and reliability obtained by DPV using (bdpy)$PW_{11}Co$/MWCNTs-COOH/GCE for the determination of IO_3^-at its various concentrations in the real samples

Sample	$[IO_3^-]$ (μM)				Recovery (%) ± SD[a] (n = 3)	
	Originally	Spiked	Proposed method	Standard method	Proposed method	Standard method
Mineral water[b]	ND[c]	5.0	4.9	5.1	99.9±1.2	100.0 ± 1.1
		10.0	9.8	10.0	99.9±1.1	100.0 ± 1.1
		15.0	15.1	15.0	100.0±1.0	100.0 ± 0.7
Tap water	ND	5.0	5.1	5.1	100.0±1.2	100.0 ± 1.1
		10.0	10.1	10.1	100.0±1.2	100.0 ± 1.2
		15.0	15.3	15.1	100.0±1.1	100.0 ± 1.1

[a]Standard deviation. [b]From local market. [c]Not detected.

4. CONCLUSIONS

A novel organic-inorganic hybrid nanocomposite modified GCE based on POM, IL, and MWCNTs-COOH has been fabricated, characterized, and developed as a capable electrocatalyst in the electrochemical detection of the iodate ion. The modified electrode revealed a notable electrocatalytic activity towards the electro-reduction of IO_3^-. The high stability, good repeatability, and reproducibility, as well as simplicity of electrode preparation, are the features of the proposed sensor. Furthermore, the modified electrode has specific characteristics such as low LOD (27.6×10^{-2} μmol L^{-1}), high sensitivity, wide linear range (10.0-1600.0 μmol L^{-1}), and good selectivity compared to other surfaces. Also, this sensor has been effectively applied for the monitoring of IO_3^- in the real samples. The results of the proposed method in real samples were in good agreement with those of the standard method. All of these beneficial properties are favorable for high-performance iodate sensors.

CONFLICTS OF INTEREST

There are no conflicts to declare.

AUTHOR INFORMATION

Corresponding Author

Somayeh Dianat: Email: s.dianat@hormozgan.ac.ir, ***ORCID***: 0000-0001-6754-4377

Author

Atefeh Karimi-Takallo

ACKNOWLEDGEMENTS

The authors gratefully acknowledge the financial support of this work by the Research Council of the University of Hormozgan.

REFERENCES

1. L. Wang, T. Meng, J. Sun, S. Wu, M. Zhang, H. Wang, Y. Zhang, *Anal. Chim. Acta*, **2019**, *1047*, 28-35.
2. Y. Tanaka, T. Hasegawa, T. Shimamura, H. Ukeda, T. Ueda, *J. Electroanal. Chem*. **2018**, *828*, 102-107.
3. M. Chi, Z. Zhu, L. Sun, T. Su, W. Liao, C. Deng, Y. Zhao, W. Ren, H. Lü, *Appl. Catal. B*, **2019**, *259*, 118089-118098.
4. Y. Jia, S. Sun, X. Cui, X. Wang, L. Yang, *Talanta* **2019**, *205*, 120139-120144.
5. Q. Huang, S. Ke, L. Qiu, X. Zhang, S. Lin, *Chem. Cat. Chem.*, **2014**, *6*, 1531-1534.
6. M. Jiang, D. Zhu, J. Cai, H. Zhang, X. Zhao, *J. Phys. Chem. C*, **2014**, *118*, 14371-14378.
7. S. Dianat, A. Bordbar, S. Tangestaninejad, S. Zarkesh-Esfahani, P. Habibi, A. A. Kajani, *J. Iran. Chem. Soc*., **2016**, *13*, 1895-1904.
8. S. Dianat, A. -K. Bordbar, S. Tangestaninejad, B. Yadollahi, R. Amiri, S. -H. Zarkesh-Esfahani, P. Habibi, *J. Inorg. Biochem*., **2015**, *152*, 74-81.
9. J. T. Rhule, C. L. Hill, D. A. Judd, R. F. Schinazi, *Chem. Rev*., **1998**, *98*, 327-358.
10. S. Omwoma, C. T. Gore, Y. Ji, C. Hu, Y. -F. Song, *Coord. Chem. Rev*., **2015**, *286*, 17-29.
11. D. -Y. Du, J. -S. Qin, S. -L. Li, Z. -M. Su, Y. -Q. Lan, *Chem. Soc. Rev*., **2014**, *43*, 4615-4632.
12. Q. Wang, J. Khungwa, L. Li, Y. Liu, X. Wang, S. Wang, *J. Electroanal. Chem*., **2018**, *824*, 91-98.
13. F. Boussema, R. Haddad, Y. Ghandour, M. S. Belkhiria, M. Holzinger, A. Maaref, S. Cosnier, *Electrochim. Acta*, **2016**, *222*, 402-408.
14. A. Proust, B. Matt, R. Villanneau, G. Guillemot, P. Gouzerh, G. Izzet, *Chem. Soc. Rev*., **2012**, *41*, 7605-7622.
15. S. Dianat, A. Hatefi-Mehrjardi, K. Mahmoodzadeh, S. Kakhki, *New J. Chem.*, **2019**, *43*, 14417-14425.

16. M. Ammam, *J. Mater. Chem. A*, **2013**, *1*, 6291-6312.
17. Y. Z. Liu, W. Yao, H. M. Gan, C. Y. Sun, Z. M. Su, X. L. Wang, *Chem. Eur. J*., **2019**, *25*, 16617-16624.
18. D. Martel, N. Sojic, A. Kuhn, *J. Chem. Educ*., **2002**, *79*, 349-352.
19. L. Adamczyk, *J. Solid State Electrochem*., **2017**, *21*, 211-222.
20. R. Ayranci, Y. Torlak, T. Soganci, M. Ak, *J. Electrochem. Soc*., **2018**, *165*, B638-B643.
21. L. Ni, G. Yang, C. Sun, G. Niu, Z. Wu, C. Chen, X. Gong, C. Zhou, G. Zhao, J. Gu, W. Ji, X. Huo, M. Chen, G. Diao, Mater. *Today Energy*, **2017**, *6*, 53-64.
22. H. Yang, T. Song, L. Liu, A. Devadoss, F. Xia, H. Han, H. Park, W. Sigmund, K. Kwon, U. Paik, *J. Phys. Chem. C*, **2013**, *117*, 17376-17381.
23. L. -H. Gao, J. -F. Zhang, H. -L. Wang, X. -Y. Lin, J. -M. Qi, K. -Z. Wang, *Electrochim. Acta*, **2015**, *166*, 215-222.
24. H. Li, S. Pang, S. Wu, X. Feng, K. Müllen, C. Bubeck, *J. Am. Chem. Soc*., **2011**, *133*, 9423-9429.
25. J. Ni, Q. -M. Fu, L. Liu, Z. -R. Gu, Z. Zhou, F. -B. Li, S. -X. Zhang, S. -Z. Liu, Z. -L. Du, *Thin Solid Films*, **2013**, *537*, 247-251.
26. C. P. Ponce, H. Y. Araghi, N. K. Joshi, R. P. Steer, M. F. Paige, *Langmuir*, **2015**, *31*, 13590-13599.
27. S. Dianat, A. Hatefi-Mehrjardi, K. Mahmoodzadeh, *New J. Chem*., **2019**, *43*, 1388-1397.
28. M. Blasco-Ahicart, J. Soriano-López, J. J. Carbó, J. M. Poblet, J. -R. Galan-Mascaros, *Nat. Chem*., **2018**, *10*, 24-30.
29. B. Suma, P. S. Adarakatti, S. K. Kempahanumakkagari, P. Malingappa, *Mater. Chem. Phys*., **2019**, *229*, 269-278.
30. W. Guo, X. Cao, Y. Liu, X. Tong, X. Qu, *J. Electrochem. Soc*., **2014**, *161*, B248-B255.
31. J. M. Cameron, D. J. Wales, G. N. Newton, *Dalton Trans*., **2018**, *47*, 5120-5136.
32. F. -Y. Yi, W. Zhu, S. Dang, J. -P. Li, D. Wu, Y. -H. Li, Z. -M. Sun, *Chem. Commun*., **2015**, *51*, 3336-3339.
33. D. -C. Zhao, Y. -Y. Hu, H. Ding, H. -Y. Guo, X. -B. Cui, X. Zhang, Q. -S. Huo, J. -Q. Xu, *Dalton Trans*., **2015**, *44*, 8971-8983.
34. E. Rafiee, F. Mirnezami, *J. Mol. Liq*., **2014**, *199*, 156-161.
35. R. Wang, D. Jia, Y. Cao, *Electrochim. Acta*, **2012**, *72*, 101-107.
36. X. Wu, W. Wu, Q. Wu, W. Yan, *Langmuir*, **2017**, *33*, 4242-4249.
37. F. Faridbod, H. Rashedi, M. R. Ganjali, P. Norouzi, S. Riahi, Application of room temperature ionic liquids in electrochemical sensors and biosensors, Intech Open Access Publisher, **2011**.
38. G. Bajwa, M. Genovese, K. Lian, *ECS J. Solid State Sci. Technol*., **2013**, *2*, M3046-M3050.
39. A. A. Ensafi, E. Heydari-Soureshjani, M. Jafari-Asl, B. Rezaei, *Carbon*, **2016**, *99*, 398-406.
40. D. M. Fernandes, M. P. Araújo, A. Haider, A. S. Mougharbel, A. J. Fernandes, U. Kortz, C. Freire, *Chem. Electro. Chem*., **2018**, *5*, 273-283.
41. L. Hong, Y. Gui, J. Lu, J. Hu, J. Yuan, L. Niu, *Int. J. Hydrogen Energy*, **2013**, *38*, 11074-11079.
42. J. Jiao, J. Zuo, H. Pang, L. Tan, T. Chen, H. Ma, J. Electroanal. Chem., **2018**, *827*, 103-111.
43. N. Thakur, S. Das Adhikary, M. Kumar, D. Mehta, A. K. Padhan, D. Mandal, T. C. Nagaiah, *ACS Omega*, **2018**, *3*, 2966-2973.
44. C. Deng, J. Chen, Z. Nie, M. Yang, S. Si, *Thin Solid Films*, **2012**, *520*, 7026-7029.
45. S. Yang, X. Liu, X. Zeng, B. Xia, J. Gu, S. Luo, N. Mai, W. Wei, *Sens. Actuators B*, **2010**, *145*, 762-768.
46. D. Zhang, H. Ma, Y. Chen, H. Pang, Y. Yu, *Anal. Chim. Acta*, **2013**, *792*, 35-44.
47. J. Hu, Y. Ji, W. Chen, C. Streb, Y. -F. Song, *Energy Environ. Sci*., **2016**, *9*, 1095-1101.
48. G. Y. Lee, I. Kim, J. Lim, M. Y. Yang, D. S. Choi, Y. Gu, Y. Oh, S. H. Kang, Y. S. Nam, S. O. Kim, *J. Mater. Chem. A*, **2017**, *5*, 1941-1947.
49. S. Liu, L. Xu, F. Li, W. Guo, Y. Xing, Z. Sun, *Electrochim. Acta*, **2011**, *56*, 8156-8162.
50. S. Iijima, *Nature*, **1991**, *354*, 56-58.
51. B. Ertan, T. Eren, İ. Ermiş, H. Saral, N. Atar, M. L. Yola, *J. Colloid Interface Sci*., **2016**, *470*, 14-21.
52. X. Kong, Y. Wang, Q. Zhang, T. Zhang, Q. Teng, L. Wang, H. Wang, Y. Zhang, *J. Colloid Interface Sci*., **2017**, *505*, 615-621.
53. S. Li, X. Yu, G. Zhang, Y. Ma, J. Yao, B. Keita, N. Louis, H. Zhao, *J. Mater. Chem*., **2011**, *21*, 2282-2287.
54. A. Manivel, R. Sivakumar, S. Anandan, M. Ashokkumar, *Electrocatalysis*, **2012**, *3*, 22-29.
55. S. Zhang, P. He, W. Lei, G. Zhang, *J. Electroanal. Chem*., **2014**, *724*, 29-35.
56. J. Zuo, N. Gao, Z. Yu, L. Kang, K. P. O'Halloran, H. Pang, Z. Zhang, H. Ma, *J. Electroanal. Chem*., **2015**, *751*, 111-118.
57. M. Sharifi, S. Dianat, A. Hosseinian, *RSC Adv*., **2021**, *11*, 8993-9007.
58. A. Karimi-Takallo, S. Dianat, A. Hatefi-Mehrjardi, *J. Electroanal. Chem*., **2021**, *886*, 115139-115151.
59. W. Song, X. Chen, Y. Jiang, Y. Liu, C. Sun, X. Wang, *Anal. Chim. Acta*, **1999**, *394*, 73-80.
60. Y. Li, W. Bu, L. Wu, C. Sun, *Sens. Actuators B*, **2005**, *107*, 921-928.
61. A. Salimi, H. MamKhezri, R. Hallaj, S. Zandi, *Electrochim. Acta*, **2007**, *52*, 6097-6105.
62. M. Zhou, L. -P. Guo, F. -Y. Lin, H. -X. Liu, *Anal. Chim. Acta*, **2007**, *587*, 124-131.
63. B. Haghighi, H. Hamidi, *Electroanalysis*, **2009**, *21*, 1057-1065.

64. B. Haghighi, H. Hamidi, L. Gorton, *Electrochim. Acta*, **2010**, *55*, 4750-4757.
65. M. Nosuhi, A. Nezamzadeh-Ejhieh, *J. Electroanal. Chem*., **2018**, *810*, 119-128.
66. J. Pishahang, H. B. Amiri, H. Heli, *Sens. Actuators B*, **2018**, *256*, 878-887.
67. F. Koohi, H. R. Zare, Z. Shekari, *Microchem. J.*, **2020**, *159*, 105425-105433.
68. M. Vithanage, I. Herath, S. Achinthya, T. Bandara, L. Weerasundara, S. Mayakaduwa, Y. Jayawardhana, P. Kumarathilaka, *Arch. Public Health*, **2016**, *74*, 21-27.
69. L. Berța, F. Boda, G. S. A, A. Curticapean, D. Muntean, *Acta Med. Marisiensis*, **2014**, *60*, 84-88.
70. P. -E. Car, B. Spingler, S. Weyeneth, J. Patscheider, G. R. Patzke, *Polyhedron*, **2013**, *52*, 151-158.
71. M. Kato, C. N. Kato, *Inorg. Chem. Commun*., **2011**, *14*, 982-985.
72. A. P. Lever, *Stud. Phys. Theor. Chem*., **1984**, *33*, 99-100.
73. A. J. Haider, M. Mohammed, D. S. Ahmed, *Int. J. Eng. Res*., **2014**, *5*, 255-261.
74. P. Nie, C. Min, H. -J. Song, X. Chen, Z. Zhang, K. Zhao, *Tribol. Lett*., **2015**, *58*, 7-18.
75. H. Ohno, Electrochemical aspects of ionic liquids, John Wiley & Sons, **2005**.
76. Z. Liu, M. Jin, J. Cao, J. Wang, X. Wang, G. Zhou, A. van den Berg, L. Shui, *Sens. Actuators B*, **2018**, *257*, 1065-1075.
77. D. Zhu, H. Ma, Q. Zhen, J. Xin, L. Tan, C. Zhang, X. Wang, B. Xiao, *Appl. Surf. Sci*., **2020**, *526*, 146721-146732.